



Does Travel Spread Infection?—Effects of Social Stirring Simulated on SEIRS Circuit Grid

Yukio Ohsawa¹ · Sae Kondo² · Tomohide Maekawa³

Received: 28 October 2023 / Accepted: 11 January 2024 / Published online: 1 March 2024
© The Author(s) 2024

Abstract

Previous models of the spread of viral infection could not explain the potential risk of non-infectious travelers and exceptional events, such as the reduction in infected cases with an increase in travelers. In this study, we provide an explanation for improving the model by considering two factors. First, we consider the travel of susceptible (S), exposed (E), and recovered (R) individuals who may become infected and infect others in the destination region in the near future, as well as infectious (I). Second, people living in a region and those moving from other regions are treated as separate but interacting groups to consider the potential influence of movement before infection. We show the results of the simulation of infection spread in a country where individuals travel across regions and the government chooses regions to vaccinate with priority. As a result, vaccinating people in regions with larger populations better suppresses the spread of infection, which turns out to be a part of a general law that the same quantity of vaccines can work efficiently by maximizing the conditional entropy H_c of the distribution of vaccines to regions. This strategy outperformed vaccination in regions with a larger effective regeneration number. These results, understandable through the new concept of social stirring, correspond to the fact that travel activities across regional borders may even suppress the spread of vaccination if processed at a sufficiently high pace. This effect can be further reinforced if vaccines are equally distributed to local regions.

Keywords Social network model · Infection spread · Travel · COVID-19

✉ Yukio Ohsawa
ohsawa@sys.t.u-tokyo.ac.jp

¹ Department of Systems Innovation, School of Engineering, The University of Tokyo, 7-3-1 Hongo, Bunkyo-Ku, Tokyo 113-8656, Japan

² Department of Architecture, Graduate School of Engineering, Mie University, 1577 Kurimamachiya-Cho, Tsu City, Mie Prefecture 514-8507, Japan

³ Trust Architecture Inc, 509, Louis Marble Nogizaka, 9-6-30 Akasaka, Minato-Ku, Tokyo, Japan

1 Introduction

The spread of COVID-19 since 2019 has involved all kinds of regions—towns, cities, prefectures, and countries—due to the movement and contact of people, even without explicit symptoms. Although testing systems at airports have been introduced and improved, further improvements are needed because the virus has spread despite these efforts (e.g., the development of governmental policies [1]). It should be noted that the first infection in a country started with a few individuals who immigrated without a positive PCR test result or any other sign of infection. Thus, borrowing words from the Susceptible-Exposed-Infectious-Recovered (SEIR) model ([2, 3] and several extensions mentioned later), attention should be paid to individuals in infection states such as exposed (E) or susceptible (S), who may change into (E) after immigration. Furthermore, we should be aware that people can travel from/to regions, such as prefectures or cities within the same country, without any tests or passport controls.

Previous studies examined the influence of travel. Statistical analyses showed that long-distance travel significantly accelerated the spread of infection. For example, countries exposed to high flows of international tourism are more prone to cases and deaths owing to the COVID-19 outbreak [4]. International tourism expenditure, international tourism receipts, international tourist arrivals, and international tourism exports were significantly correlated with the total number of cases, daily growth of COVID-19 cases, and number of cases, especially in places with high incomes [5]. Using network- or population-based models of the spread of infection, long-distance movement across regions has been shown to cause a significant increase in the number of infected individuals [6–8]. This finding can be related to the lesson *Stay with Your Community* (SWYC [9]) for suppressing the spread of infection learned from simulations on a social network model. SWYC means that each individual should avoid meeting as many other unintended people as people to meet intentionally, because the excess triggers an explosive spread of infection. The risk of long-distance travel is regarded as the risk of meeting unintended people. However, we obtain a surprising tendency by combining recent data in [10] and [11], where we find that the increase in the number of travelers and new infection cases co-occurred until close to the end of 2020; however, their trends started to correlate negatively, as shown in Fig. 1. That is, people in the USA started to travel frequently from the beginning of 2021, 2 weeks after the start of vaccination, but the number of new cases was suppressed. Statistical analyses of the temporal changes obtained results correspond to such an observation: a statistically significant, although small, relationship between immigrant flows and COVID-19 rates in border counties existed, but the increase in local cases became non-significant with increasing local vaccination rates [12]. Other results indicate that travel restrictions to and from the country only modestly affect the epidemic trajectory unless combined with additional measures, such as the reduction of transmission in the community [13].

In this paper, we present *SEIRS circuits Grid* to solve the problem of *interregional community confusion*—movements due to interregional travel

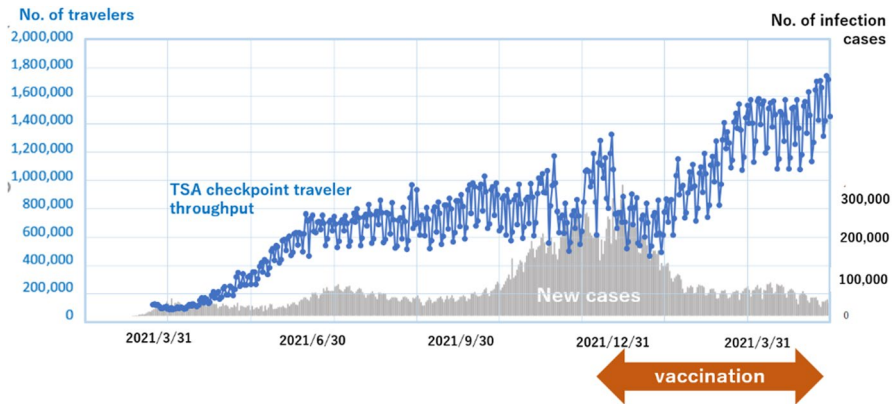


Fig. 1 An example of downtrend of COVID-19 infection cases in US after introduction of vaccines in spite of the uptrend of travel activities

cause complex interactions between individuals from multiple communities and regions. Here, individuals in states S , E , I , or R traveling from one region to another are dealt with as different groups, but may come into infectious contact with those in the destination region. The new method is presented in Sect. 2. In Sect. 3, we present the settings for simulations based on the SEIRS circuit grid in Sect. 4. The results in Sect. 4 will be discussed in Sect. 5, where the concept of *social stirring* is introduced to explain observed phenomena, such as the effects of activated travel on the suppression of infection cases at a higher rate of vaccination.

2 Grid of SEIRS Circuits

2.1 The SEIR Model and Extensions

In the susceptible–exposed–infectious–recovered (SEIR) model [14–16], S , E , I , and R refer to the following numbers of people:

S : number of *susceptible* individuals. When a susceptible individual comes in contact with a risk of infection (e.g., 15 min within a distance of 2m), the susceptible individual may catch the virus and transition to E below.

E : The number of individuals who have been *exposed* but are in an incubation period during which one may have caught the virus, but is not yet infective.

I : Number of individuals who have been infected and may have infected individuals in S .

R : Number of individuals *recovered* from State I . Some analysts deal with dead individuals as a part of R (called *removed* in such a case), but below, we count the dead as a part of I who do not transit to R .

The SEIR model has been used with the daily number of passengers using public transportation to determine the effects of human mobility restrictions [17, 18].

According to analyses using the SEIR model, mobility restrictions for individuals with symptomatic infections and high-risk regions had substantial effects on reducing the spread of COVID-19; for example, a 4-week delay of spread if two high-risk regions were locked down [18]. The SEIR model was extended to decompose the transmission of COVID-19 into cases induced by residences and facilities, using mobility data [19]. SEIR has been further extended to reflect the factors influencing the pattern of infection spread in each country, such as interregional travelers [20] and the age of the population [21]. A modified SEIR model has also been proposed to assess the effectiveness of social distancing, banning gatherings, and vaccination strategies [22]. However, the problem addressed below, called *interregional community confusion*, has not been explicitly highlighted.

To include the influence of travelers from other regions, the number of infective people was previously represented by I_{in} , which indicates the risk in a region due to receiving travelers [20]. Thus, Eqs. (1)–(4) were used as the analysis models to simulate the spread of infection. See Fig. 2a for an illustration of the model. If we reflect only the infected influx, as in I_{in} , it disables the consideration of exposed but not yet infected individuals, who should be represented by E_{in} . Table 1 presents the variables used in this study

$$\frac{dS}{dt} = m_{SER}(N - S) - r_3S(I + I_{in})/N \quad (1)$$

$$\frac{dE}{dt} = -(r_1 + m_{SER})E + r_3S(I + I_{in})/N \quad (2)$$

$$\frac{dI}{dt} = -(r_2 + m_I)I + r_1E \quad (3)$$

$$\frac{dR}{dt} = -m_{SER}R + r_2I. \quad (4)$$

2.2 SEIRS Circuit Grid to Solve the Interregional Community Confusion

To reflect the exposed influx and represent the return of people in R to the S state, as in the SEIRS model owing to the loss of once-acquired immunity [23, 24] by r_4 , we consider the model given by Eq. (5)–(8) as shown in Fig. 2b. S_{in} , E_{in} , I_{in} , and R_{in} refer to the influx of travelers to be merged in the target region with others in S , E , I , or R

$$\frac{dS}{dt} = S_{in} + r_4R + m_{SER}(N - S) - r_3SI/N \quad (5)$$

$$\frac{dE}{dt} = E_{in} - (r_1 + m_{SER})E + r_3SI/N \quad (6)$$

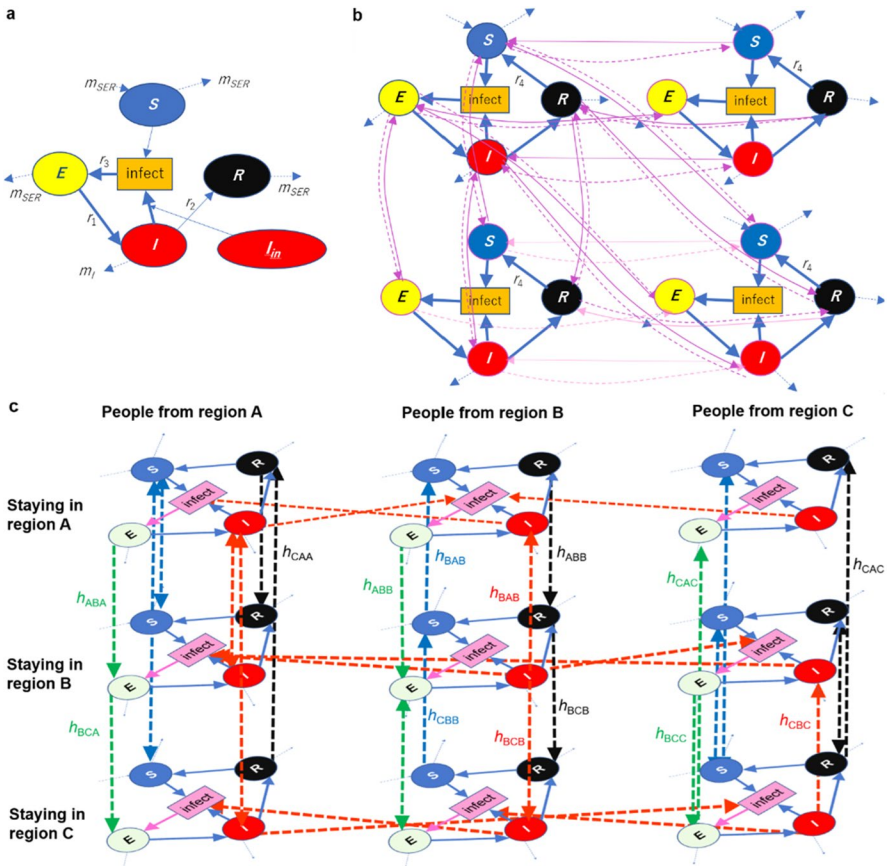


Fig. 2 Three SEIR-based models. **a** SEIR considering the number of infective influx travelers (I_{in}) in the region receiving travelers, corresponding to Eq. (1)–(4). The italicized letters show the variables and parameters in these equations. **b** The movement of S , E , I , and R with travel, having a circuit where people return from R to S due to the loss of acquired immunity corresponding to Eqs. (5)–(8) including parameter r_4 . The other parameters are succeeded from **a**. The bottom figure **c** SEIRS circuit grid where vertical alignment of the SEIR circuit shows the movement of people from the same region and horizontal the interaction of people in a region corresponding to Eqs. (11)–(14). h_{ijk} is equal to $\alpha T_{ij} / N_{ki}$ i.e., the percentage of travelers from i to j among those who came from k to i . The other parameters are succeeded from **a** and **b**

$$\frac{dI}{dt} = I_{in} - (r_2 + m_I)I + r_1E \tag{7}$$

$$\frac{dR}{dt} = R_{in} - (r_4 + m_{SER})R + r_2I. \tag{8}$$

However, we consider a problem that we call *interregional community confusion*: movements due to interregional travel cause more complex mutual interactions between individuals from multiple regions than a one-way transition. For example,

Table 1 Variables referred to from multiple sections in this paper

N_{ij}	The number of people originating from region i and staying in j
$S_{ij}, E_{ij}, I_{ij}, R_{ij}$	The number of susceptible, exposed, infective, or recovered individuals originating from region i and staying in j . $S, E, I,$ and R are called states. The suffixes of states are cut in Fig. 2c appearing later for simplicity
$s_{ij}, e_{ij}, \psi_{ij}, r_{ij}$	The division of $S_{ij}, E_{ij}, I_{ij}, R_{ij}$ by N_{ij}
$R_i (R_{ij})$	The effective reproduction number (in region j); R_i is the average of R_{ij} for all regions (j 's) in the country
R_{vac}	The average of R_{ij} for all j 's weighted by the number of vaccinated individuals in region j : Note this is not the sheer effective reproduction number of the country
T_{jk}	The number of travelers from prefecture j to k per day in a normal year when COVID-19 did not appear yet, i.e., 2019 and before
$r_1 (r_{1i})$	The percentage of individuals to be infective per day, among exposed ones (who originate from region i)
$r_2 (r_{2j})$	The percentage of recovering individuals per day, among infective ones (who stay in region j)
$r_3 (r_{3j})$	The percentage of contacts which cause infections (in region j). $r_3 = c R_i$ where c is a constant value
$r_4 (r_{4i})$	the percentage those who return to the susceptible, among recovered ones (who originate from region i)
m_I	the death rate of infective individuals
m_{SER}	the death rate of individuals in $S, E,$ or R states
$p_v (p_{vj})$	the percentage of vaccine dozes per day in the entire national population (the population of region j)
H_c	the conditional entropy of vaccine distribution to all regions
α	traveling activity, that is the number of travelers compared with the normal year (2019), supposed to be uniform in the entire nation

suppose that only two regions, A and B, exist for simplicity, where a certain number of individuals from region A travel to region B and stay there for a few days. As these travelers are expected to return to region A, the change in the number of individuals in all states in B depends on the difference between the densities of $S, E, I,$ and R in travelers from A to B and those returning from B to A after being assimilated with others in B to A, as represented in Eq. (9). Here, it is assumed that the same number of people, T_{AB} , who travel to region B return to region A. If the returning people are supposed to acquire the states of the others in B, X_{Bin} in Eq. (9) indicates the added number of members in State B of State X ($S, E, I,$ or R). Here, N_A represents the number of people in A and X_A represents the number in state X in region A

$$X_{Bin} = \left(\frac{X_A}{N_A} - \frac{X_B}{N_B} \right) T_{AB}. \quad (9)$$

Thus, X_{Bin} reflects the difference between the densities of the population in state X in regions A and B, where X_B/N_B (or X_A/N_A) is regarded as the density of state X among all who return to region A from B (or go out to region B from A), assuming that travelers succeed in the state of people in the region from which they move.

However, it is mostly just a few days (2.3 days on average in Japan, estimated on the assumption that a traveler goes to one place at once per day [25], which coincides with the computed average in [26]) between the time travelers go from region A to B and the time they return to A. During such a short period, the ratio of travelers in state X changes by an incomparably smaller value than X_A/N_A . This can be expressed as follows:

- The number of travelers from region A to region B: ρN_A .
- Number of travelers in state X from region A to region B: ρX_A .
- Travelers returning to region A from region B: $(1\delta_1 -) \rho N_A$.
- Travelers returning to region A from region B in state X : $(1 + \delta_2) \rho X_A$.

Here, ρ denotes the ratio of travelers from A to B among all in A, δ_1 the ratio of travelers who stay longer in B than those who return in a few days to A, and δ_2 the ratio of those who newly enter state X (newly infected minus those who recover if X is I) within a few days. Equation (9) is replaced by Eq. (10), which shows X_{Bin} is significantly smaller than $X_A T_{AB}/N_A$ because $|\delta_1| \ll 1$ and $|\delta_2| \ll 1$.

$$X_{Bin} = - \left(\frac{\delta_1 + \delta_2}{1 - \delta_1} \right) \frac{X_A}{N_A} T_{AB} \tag{10}$$

However, if regions A and B are significantly different, X_{Bin} in Eq. (9) is comparable to that of $-X_B T_{AB}/N_B$. Owing to the gap between Eq. (9) and the corrected Eq. (10), equation set [Eqs. (5)–(8) or Fig. 2b)] cannot fit real travel activities. To cope with this problem, we propose a model in which individuals in states $S, E, I,$ or R , traveling from region A to B, are treated as different groups from the others in B but may come into infectious contact. When they return from regions B to A, their probability of being in state X should be estimated to be close to X_A/N_A instead of X_B/N_B . Thus, we considered these two effects by extending the SEIRS circuit in Fig. 2b to the grid structure in Fig. 2c.

- i) Infected individuals in B may infect others staying in B, including those traveling from other regions.
- ii) An individual traveling from A to region B is added to the group of other individuals in the same state as oneself, staying in B, and coming from A.

Consequently, the model developed in this study is represented by Eqs. (11)–(14).

$$\frac{dS_{ij}}{dt} = \alpha \sum_k (s_{ik} T_{kj} - s_{ij} T_{jk}) + r_{4i} R_{ij} - r_{3j} \frac{\sum_k S_{ij} I_{kj}}{N_j} - \nu p_{vj} N_{ij} \tag{11}$$

$$\frac{dE_{ij}}{dt} = \alpha \sum_k (e_{ik} T_{kj} - e_{ij} T_{jk}) - r_{1i} E_{ij} + r_{3j} \frac{\sum_k S_{ij} I_{kj}}{N_j} \tag{12}$$

$$\frac{dI_{ij}}{dt} = \alpha \sum_k (\psi_{ik} T_{kj} - \psi_{ij} T_{jk}) + r_{1i} E_{ij} - (r_{2j} + m_i) I_{ij} \tag{13}$$

$$\frac{dR_{ij}}{dt} = \alpha \sum_k (r_{ik}T_{kj} - r_{ij}T_{jk}) + r_{2j}I_{ij} - r_{4i}R_{ij}. \quad (14)$$

The first term $x_{ik}T_{kj}$ on the RHS of each equation, with dX_{ij}/dt on the LHS, corresponds to those who come from region i to j via k . Here, the number of people who travel from k to j is multiplied by the proportion of those from i to k in state X . The second term $x_{ij}T_{jk}$ considers those who leave j for k in state X among those in j who come from i .

Here, we set m_{SER} to zero and ignored the terms that vanished. About the parameter values in Eqs. (11)–(14), we set α to 1 for the most recent normal year, 2019. Assuming a decrease of 60% in 2021 compared with 2019 (on the statistical data [27, 28]), α , which is the traveller's activity, of 0.4 is regarded as approximating the current status. T_{kj} was obtained from the approximate frequency of movement within each region (prefecture) and from each region to other regions in an ordinary year before 2020 based on the reference data in [26]. Specifically, $2.3T_{1j} + T_{2j}$ is obtained by referring to this dataset for T_{1j} meaning the number of travelers who stay in region j (for 2.3 days as mentioned above) on average and T_{2j} of a 1-day trip. This value for each region (i.e., j) is then divided into T_{kj} , which represents the movement from each region (k) in proportion to the population of the destinations (k).

Borrowing the idea from existing models of infection spread with vaccination [20, 22, 29–32], we integrated the doses of vaccination into the reduction of S as in Eq. (11), with p_{vj} as the pace of vaccination in region j (the ratio of individuals vaccinated per day in the population of region j ; to avoid confusion with the percentage of already-vaccinated individuals, here we call vaccination pace instead of rate). p_v without suffix j denotes the ratio of the number of vaccinated individuals per day to the entire national population. v is the efficiency of the vaccine in reducing susceptibility. α is the ratio of the number of travelers to that before 2020.

Thus, challenging the interregional community confusion, we obtained an extended model called the Grid of SEIRS circuits, as shown in Fig. 2c, to reflect the interregional travel without the confusion of permanent habitants and individuals from/to other regions suffered in the model shown in Fig. 2b. Each vertical alignment (i.e., column) of the SEIR circuits is linked by vertical arrows in Fig. 2c, which show the movement of people originating from the same region. In this movement, individuals embrace states S, E, I, or R, which change via interactions between people originating from various regions and meeting within a region, as indicated by the horizontal arrows.

3 The Setting for Simulations

We performed simulations by considering the virus variant VOC-202012/01 (lineage B.1.1.7). Here, r_1 was set equal to 0.2, r_2 to 0.1, r_3 to $0.1 \cdot R_t$, and m_1 to 0.012, close to the real death rate of infected cases of COVID-19 in Japan. r_4 was set to 0.002 based on a previous study [24]. The value of R_t on the first day 7th April in the simulated period was set equal to the value on the same date in 2020 [33] and magnified linearly by 40% for the 50 days from April 2021 according to the

increase in the values of R_i for variants according to the literature (an increase of 32% [34], 43–90% [35], etc., according to the literature). The vaccine is supposed to reduce the infectivity by 30% and 80% by the first and second doses, respectively, to obtain ν of 55% in Eq. (11). Note that the aim of this study is to show a general tendency regarding the spread of infection and strategies for its control using a vaccine, rather than quantitatively correct predictions. However, to show the generality of the discovered tendencies, we also present the results for B.1.617 (delta variant [36–38]). Omicron variants are beyond the scope of this study because of their extraordinarily rapid mutation, strong reduction in antibody neutralization, and enhanced infectivity [39].

The initial values of S_{ij} , E_{ij} , I_{ij} , and R_{ij} are given by Eqs. (15)–(19), Δt_1 , Δt_2 , Δt_3 , H_i , r_{4i} , and γ are constant values, and all other terms are functions of time t . Δt_1 , Δt_2 , and Δt_3 are set to 2, 14, and 448 days, respectively. γ , the number of days to stay when one travels is set to 2.3. Function infecting (t) represents the number of newly infected cases on day t (data from NHK [40]).

$$N_{\text{base } ij}(t) = \gamma T_{ij}(t), \tag{15}$$

$$E_{ij}(t) = N_{ij}(t)/N_{ii}(t) \text{avr}_{\tau \text{ in } [t-\Delta t_1-2:t-2]} \text{infect}_i(\tau)/r_{1t}, \tag{16}$$

$$I_{ij}(t) = N_{ij}(t)/N_{ii}(t) \sum_{\tau \text{ in } [t-\Delta t_2-2:t-2]} \text{infect}_i(\tau), \tag{17}$$

$$R_{ij}(t) = (1 - r_{4i})N_{ij}(t)/N_{ii}(t) \sum_{\tau \text{ in } [t-\Delta t_3-2:t-2]} \text{infect}_i(\tau), \tag{18}$$

$$S_{ij}(t) = N_{ij}(t) - \{E_{ij}(t) + I_{ij}(t) + R_{ij}(t)\}. \tag{19}$$

4 Results

4.1 The Effects of Selecting One Prefecture to Vaccinate

The results with p_v equal to 1% are shown for the simulated year from April 2021 to March 2022 in Fig. 3a–c, where one prefecture to be vaccinated was selected for each curve representing a sequence of the number of infections. In Fig. 3d, e, the population of the vaccinated prefectures and the number of accumulated infections are plotted for each of the 47 sequences, vaccinating a selected prefecture for one sequence.

As in the comparison between vaccinating people only in Tokyo and Hyogo in Fig. 3b, c, choosing a region with a larger population for vaccination causes a stronger suppression of the spread of infection. Figure 3d, e clarifies this tendency; the Pearson’s correlation R between the population of the selected prefecture for

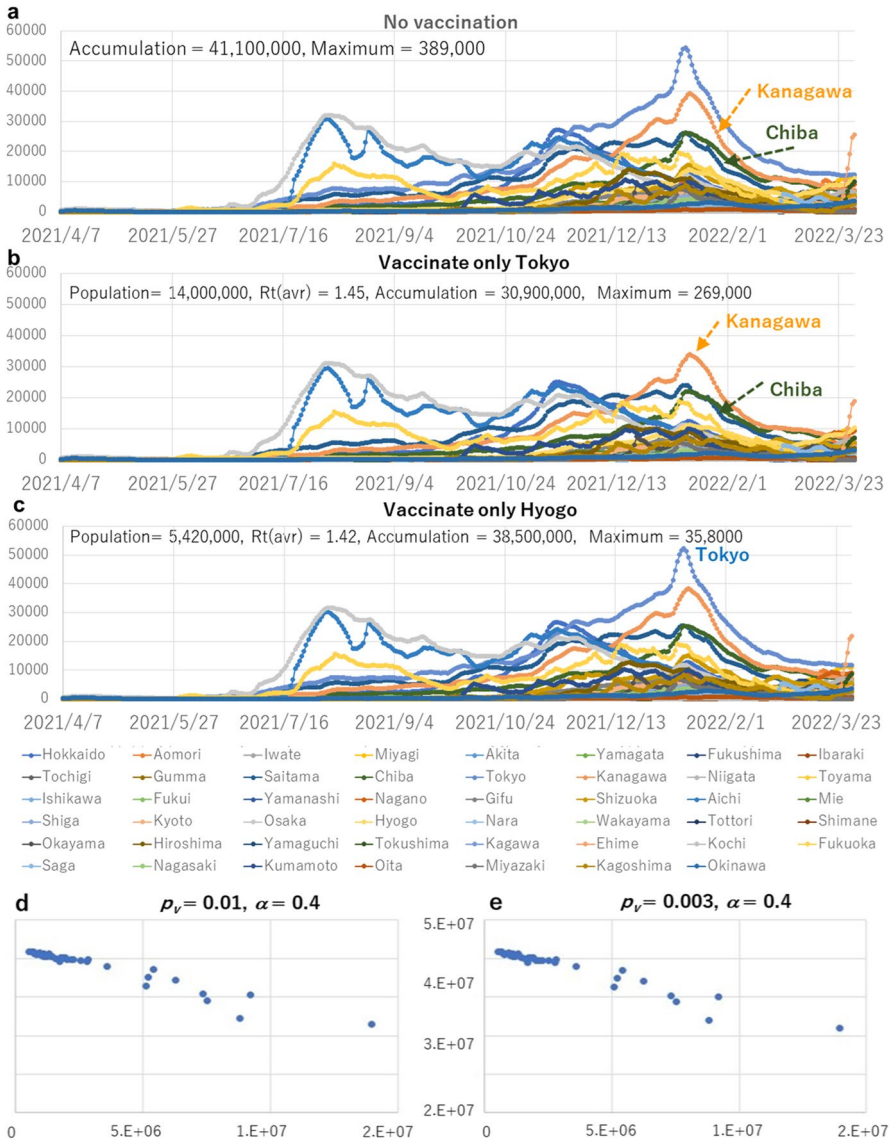


Fig. 3 The results of vaccinating no or a selected prefecture. **a** no vaccination, **b** vaccinating 0.3% of the national population per day, i.e., $p_v = 0.3\%$, selecting Tokyo (population 1.4×10^7 , $R_t = 1.45$) and **c**: Hyogo (5.4×10^6 , 1.42). α was set to 40% which is realistic in 2021 according to the data from May 2021. **d** ($p_v = 0.3\%$) and **e** ($p_v = 0.1\%$): the number of accumulated infections (vertical) versus the population of vaccinated prefectures (horizontal)

vaccination and the accumulation of infection cases is -0.969 and -0.972 for p_v of 0.3% and 1% respectively.

4.2 Conditional Entropy of Regional Distribution of Vaccines and the Effect of Movements from/to Prefectures

To investigate the effects of travellers’ activities, we show cases in which vaccines are distributed across multiple prefectures. The diversity in the distribution of vaccines to prefectures can be represented by the conditional entropy H_c defined in Eq. (20). In Eq. (20), e_i ($i \in \{0, 1\}$) denotes an event in which an individual is vaccinated for $i=1$ but not for $i=0$, and C_j ($j \in \{0, 1, \dots, \text{thenum.ofregions} - 1\}$) indicates that the individual was vaccinated in the j th region. $p(e_1|C_j)$, $p(e_0|C_j)$, $p(e_1, C_j)$, $p(e_0, C_j)$ are equal to p_{vj} , $1 - p_{vj}$, $p_{vj}N_{jj}/N$, $(1 - p_{vj})N_{jj}/N$. N represents the entire national population

$$H_c = - \sum_{i,j} p(e_i, C_j) \log p(e_i|C_j). \tag{20}$$

Conditional entropy, which is prevalent in the selection of variables in machine learning, refers to the extent to which vaccines are distributed diversely without a specific intention or causality when choosing a region to vaccinate.

Each sub-figure in Fig. 4a–l shows a simulated sequence of the number of infection cases, setting a pair of values (p_v, α) . a–d: without vaccination, e–h: $p_v=0.4\%$ of the national population per day, i–l: $p_v=1\%$. Here, we observed the effect of suppressing the spread by accelerating vaccination (increasing p_v). From the comparison of Fig. 4a–d, e–h, and i–l, we found that the increase in α tends to enhance infections in the low range of p_v . In particular, infections in local regions, such as Kumamoto, Ehime, and Okayama, rather than Tokyo or Osaka, have increased. However, this tendency is reversed for the larger value of p_v as 1.0 (i through l here). In Fig. 4m, n, we compare the accumulated infection cases for the sequences of various values of H_c .

The sequences of infected cases corresponding to the arrows in Fig. 4m are shown in Fig. 5 for various values of conditional entropy H_c , for a fixed total vaccination p_v and constant travel activity α . As shown in Fig. 5, the distribution of vaccines with larger H_c values tended to result in a more substantial suppression of the spread of infection.

Figure 6a–l shows the effect of conditional entropy H_c on the number of infection cases of B.1.1.7. These figures were obtained by varying the vaccination pace p_v from 0 to 1% and α from 0.13 to 2.0, collecting 100 sample sequences for each condition given by a pair of (p_v, α) , randomly setting p_{vj} of each (j th) region, which is the percentage per day of vaccinated individuals among the population of the region. Here, we use $\sum_j p_{vj}N_{jj} = p_v \sum_j N_{jj}$, that is, the total number of vaccines used per day in the entire country is given by the percentage of vaccination relative to the national population. As a result, the increase in H_c was negatively correlated with the number of infection cases in each condition. This tendency ranges from moderate to strong negative correlations (Pearson’s coefficients R ’s in the subfigures range

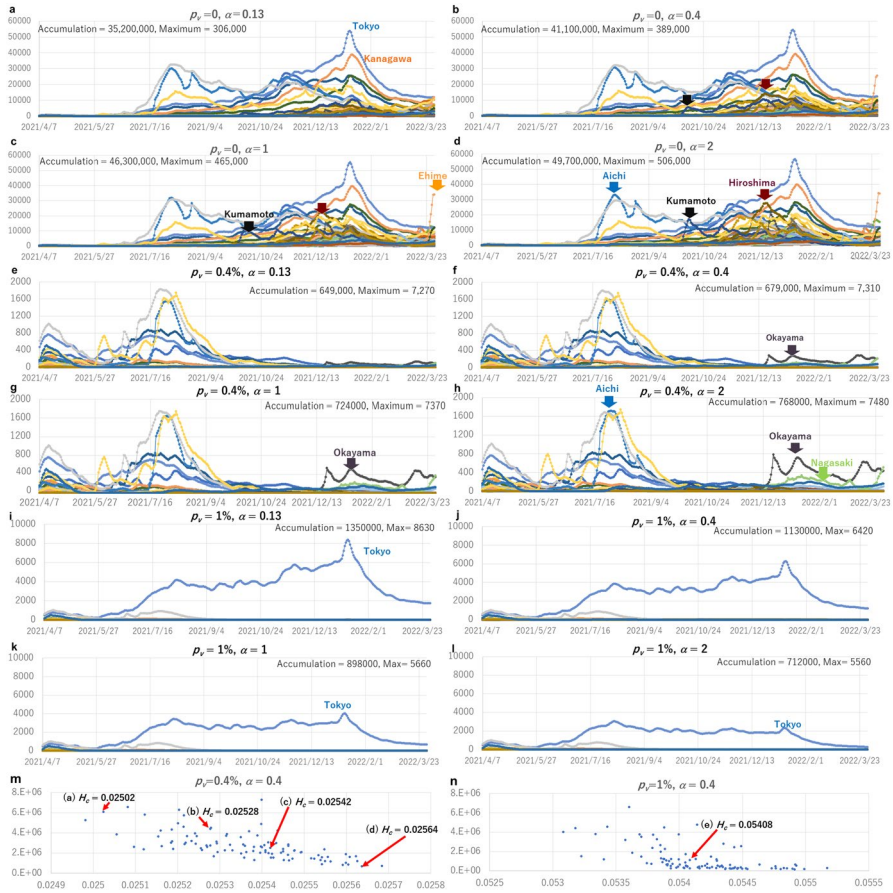


Fig. 4 a–d Newly infected cases per day for different activities α ’s of travelers without vaccination; e–h the results for the activities of travelers for $p_v = 0.4\%$ of the national population per day, as (d) of the largest H_c among (a, b, c), and (d) in m. On the other hand, i–l are the results for the activities of travelers for $p_v = 1\%$ of the national population per day, of the middle-valued H_c in n. Here, m and n show the total accumulated cases of all prefectures in 100 sequences for various H_c , represented by 100 dots for the two values of p_v .

between close to -0.5 and over -0.7) for p_v of 0.2% and larger, as shown in Fig. 6. In addition, an increase in α tends to enhance infections in the low range of p_v , and this tendency is reversed for a larger range of p_v .

On the other hand, to validate the expectation that the average effective reproduction number of vaccinated regions can be a measure of the effect of vaccines, the dependency of the accumulated number of infection cases on R_{vac} representing the average of effective reproduction number R_{ij} for all regions (i.e., j ’s), weighted by the number of vaccinated individuals, is shown in Fig. 7a–l, varying the vaccination pace p_v and travel activity α . Note that Fig. 7 does not show the correlation of the spread with the R_i of the country, averaging R_{ij} for all j , but shows a correlation with

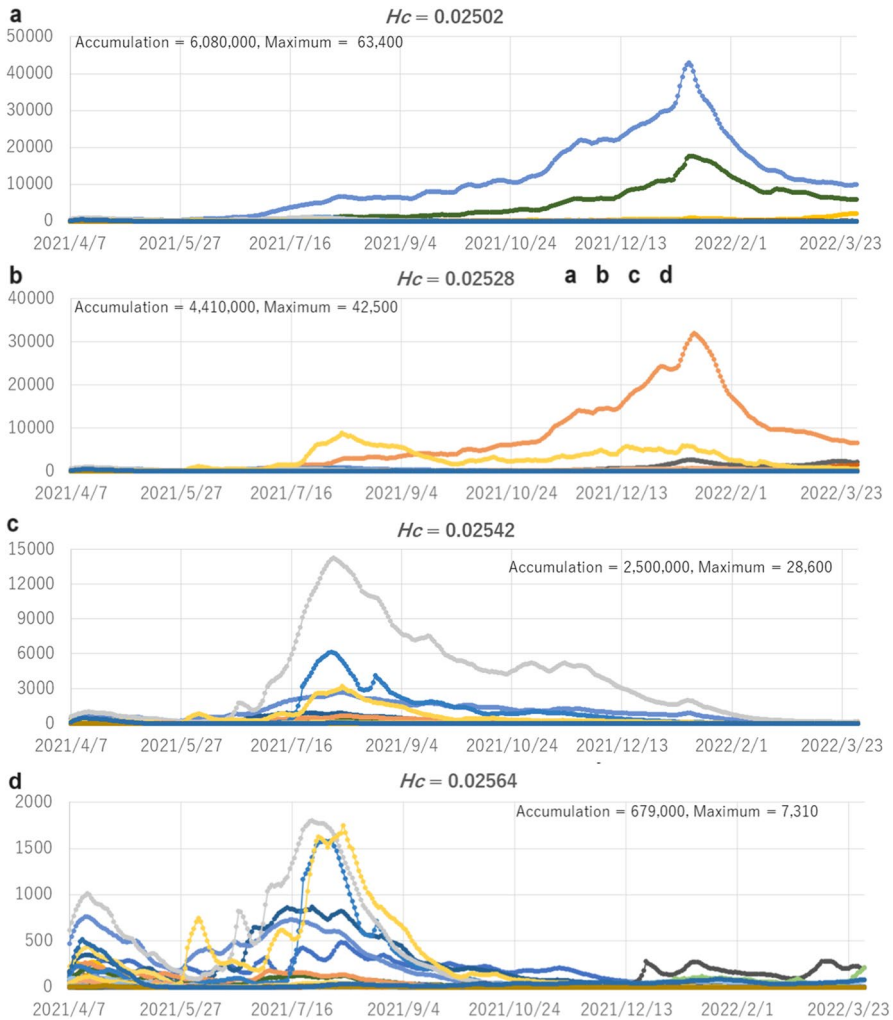


Fig. 5 Sequences of daily infected cases for varied values of conditional entropy H_c for a fixed total vaccination $p_v=0.4\%/day$ and constant travel activity $\alpha =0.4$. The sequences correspond to the arrows in Fig. 4m. The vertical axis shows the obvious reduction of infected cases for larger H_c

R_{vac} , the average of R_{ij} of regions where the government aimed to strongly suppress the spread. Therefore, a negative correlation is expected. By comparing Figs. 6 and 7, we find that the dependency of the vaccination effect on H_c is more significant than that on R_{vac} . The Pearson’s correlations in the figures support this observation.

In Fig. 8a, the effect of p_v on the average number of infection cases (accumulation) for α of 0.13, 0.3, 1.0, and 2.0 is shown. Information about errors, such as standard deviations or confidence intervals, are not included in Fig. 8a but are in Fig. 8b where the p value as a result of the t test is shown on the vertical axis as an index of the significance of the effect of α on the number of infection

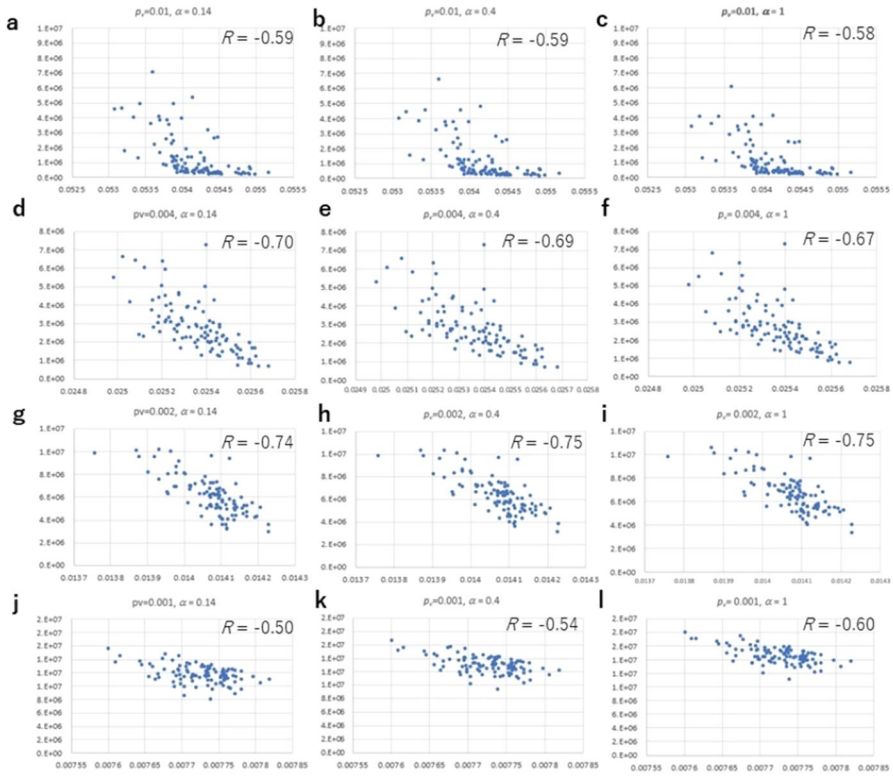


Fig. 6 The effect of conditional entropy H_c (horizontal) on the number of infection cases (accumulation, vertical axis) of B.1.1.7, varying vaccination pace p_v and travel activity α

cases for each value of p_v . For example, the p value for $\alpha=2$ was obtained to evaluate the significance of the difference in the number of infections between two conditions: $\alpha=1$ and $\alpha=2$. Although a p value is usually used to discretely check the significance by comparing it with a borderline value (e.g., $p < 0.05$); here, we use a smaller p value as evidence of a more significant difference. Here, we find a noteworthy tendency regarding the traveling activity. That is, more frequent travel across the borders of prefectures, represented by the larger α causes a greater increase in the number of infected cases below the vaccination pace p_v of 0.1%. However, the increase is moderate as p_v is improved to close to 0.4% and decreases if p_v is further increased to close to 1%. As shown in Fig. 8a, p_v of approximately 0.4% is the borderline for this reversal. As shown in Fig. 8b, the suppression of infection spread with an increase in α was found for $p_v > 0.4%$ but was not as significant as the acceleration with an increase in α for $p_v < 0.3%$.

In Figs. 9, 10, 11, we present the results for B.1.617 (the delta variant), setting it to reach an increase in R_t of 27% from the 51st to the 100th day of the simulated period. In Fig. 9, for the cases with B.1.617, similar to Fig. 6, we observe a dependency of the number of infection cases on H_c . The negative correlation of

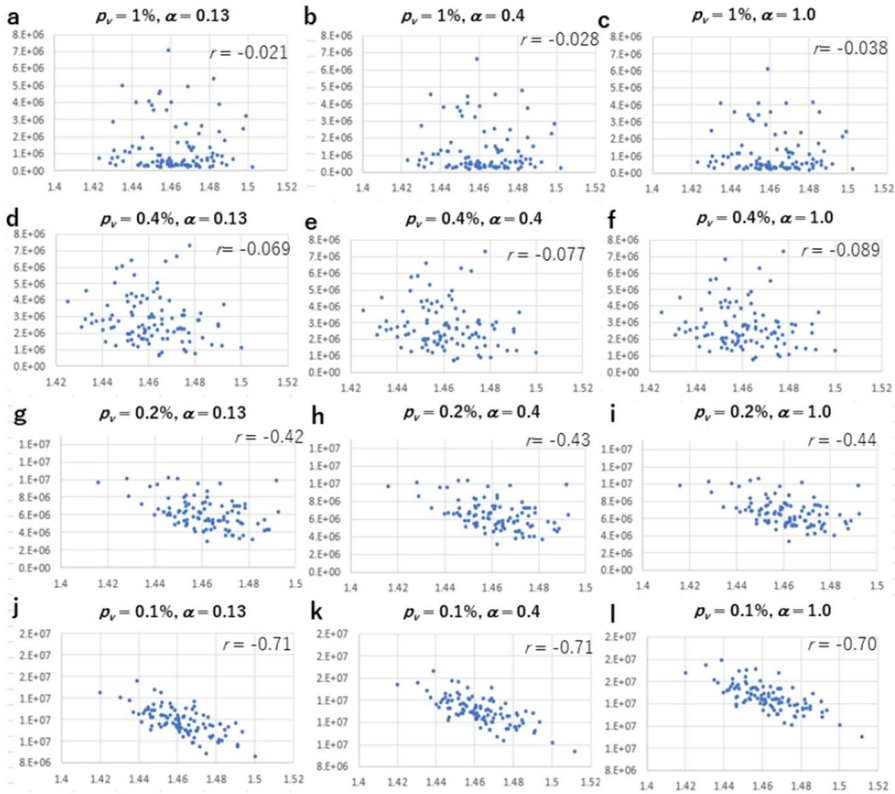


Fig. 7 The effect of R_{vac} (weighted average of R_{ij} for vaccinated regions) on the number of infection cases (accumulation of B.1.1.7), varying vaccination pace p_v and travel activity α

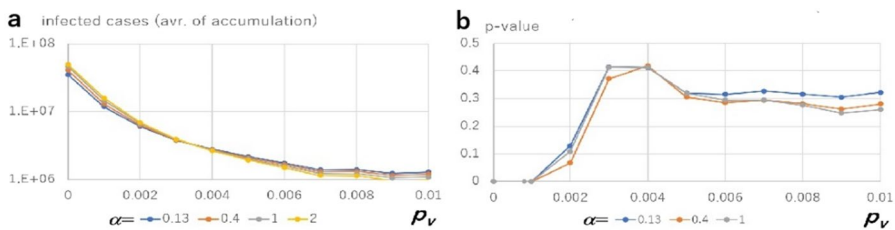


Fig. 8 The effect of vaccination pace p_v on the average number of infection cases (accumulation of B.1.1.7) for α of 0.13, 0.3, 1.0, and 2.0 is shown in **a**. In **b**, the p value as a result of the t test is shown on the horizontal axis as an index of the significance of the effect of α on the number of infection cases for each value of p_v .

the number of infection cases with H_c for $p_v > 0.2\%$ is here found to be more significant for B.1.617. In Fig. 10, the positive correlation of the number of infected cases with the average R_{vac} in the case of $p_v = 0.1\%$ for B.1.617 was negative, as expected for B.1.1.7. The correlations for other values of p_v were even lower in

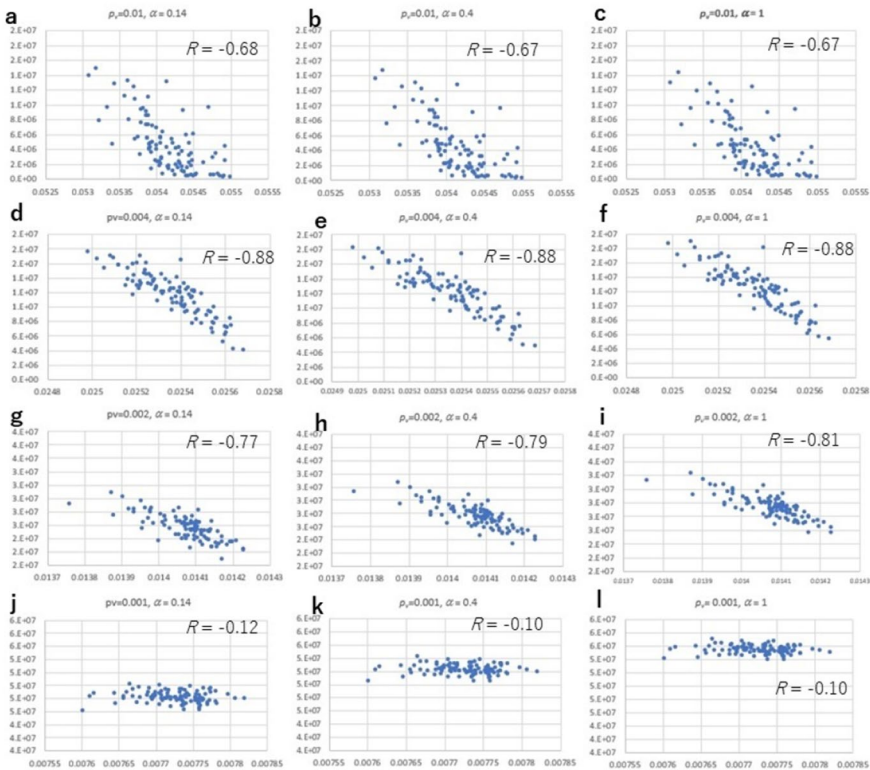


Fig. 9 The effect of conditional entropy Hc on the number of infection cases (accumulation), varying the vaccination pace p_v and the travel activity α , in the case of the variant B.1.617 (Delta variant)

Fig. 10 than in Fig. 7. Finally, as shown in Fig. 11, for cases of B.1.617 corresponding to Fig. 8 of B.1.1.7, the suppression of infection spread for an increase in α was found for $p_v > 0.6\%$, although it was not as significant as the acceleration with an increase in α for $p_v < 0.5\%$. This tendency was similar to that shown in Fig. 8. These results are referred to in the discussions in Sect. 5.

5 Discussion

5.1 The Overall Observations of the Results

The tendency is shown in Fig. 3, and the spread of infection is suppressed when a prefecture with a larger population is selected for vaccination, which may be counterintuitive, because the number of vaccinated individuals was equal in all simulated cases. However, it is natural that the spread in the prefectures selected for vaccination is substantially suppressed; therefore, the above tendency is comprehensible.

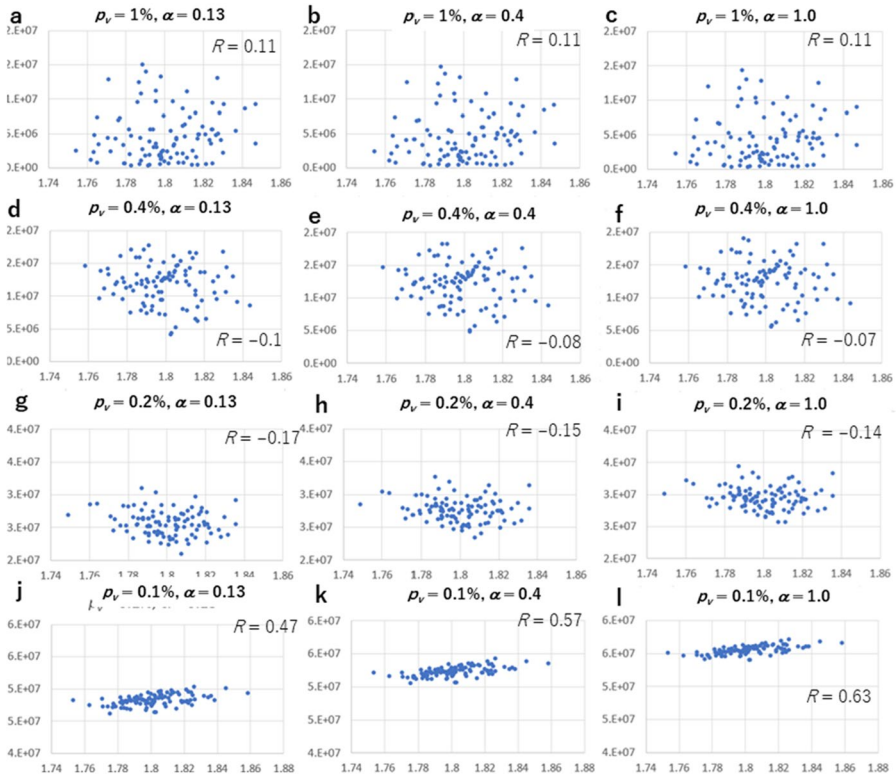


Fig. 10 The effect of effective reproduction number on the number of infection cases (accumulation), varying the vaccination pace p_v , and the travel activity α , in the case of the variant B.1.617

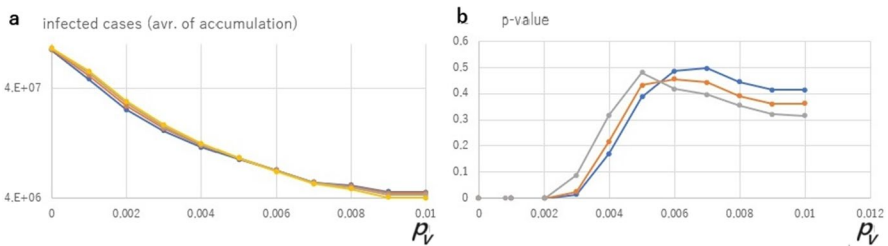


Fig. 11 The effect of vaccination pace p_v on the average number of infection cases (accumulation) for α of 0.13, 0.3, 1.0, and 2.0 is shown in **a**. In **b**, the p value as a result of the t test is shown on the horizontal axis, as an index of the significance of the effect of α on the number of infection cases for each value of p_v , in the case of the variant B.1.617

On the other hand, as shown in Fig. 4, even the tendency of enhancement of the spread in local regions due to the activation of travel (increase in α) was reversed by accelerating the vaccination pace, i.e., for the larger p_v , which is an essential finding

in this study. In addition, the larger the value of H_c , the more efficient the vaccination results in suppression, as shown in Figs. 4m–n, 5, and 6.

The above observations can be explained by introducing the social network shown in Fig. 12; a conceptual illustration of networks of infectious contacts was manually generated by the author, where the solid lines show the infectious connections (contacts) among individuals represented by nodes. As shown in Fig. 12a, the infective connections without disturbance by vaccinated individuals caused the infection to spread across the regions. If the vaccines are distributed equally to regions corresponding to a large H_c , the infection spread is suppressed and the range of nodes infected owing to the spread from each initially infected individual (nodes with thick rims) becomes narrower, as shown in Fig. 12b. However, if infected (infected and not yet recovered) individuals travel across regions, the *social stirring* of non-vaccinated individuals by traveling across regions causes a faster reproduction that corresponds to the change from Fig. 12a–c. In contrast, the social stirring caused by vaccinated individuals traveling across regions causes a slower pace of reproduction because of the elimination of infectious interregional connections. If the vaccines are distributed to multiple prefectures unequally, that is, at a low or moderate value of conditional entropy H_c , as shown in Fig. 12a, this type of social stirring is expected to increase H_c with a cutting-off effect over the entire network, as shown in Fig. 12d.

This explanation is consistent with the results shown in Fig. 4a–h, where the travel of non-vaccinated or weakly vaccinated individuals spread the virus to foster infection. On the other hand, Fig. 4i–l, which may be surprising in that frequent travels are found to suppress the spread of infection, are also explainable, because

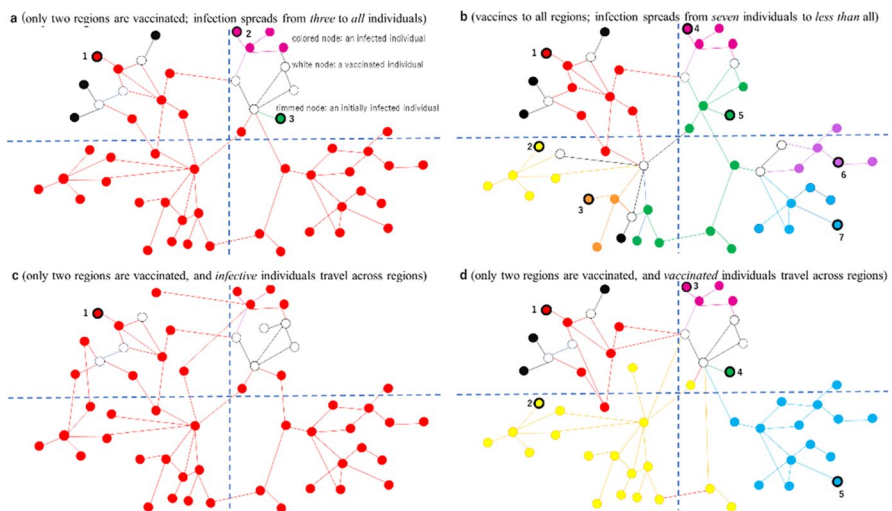


Fig. 12 A conceptual illustration of networks of infectious contacts, manually generated by the author: the white nodes represent vaccinated individuals, segmenting regions by dotted lines. **a** the spread due to the vaccination in few regions, **b** the spread suppressed due to vaccines distributed equally to regions, **c** fostered spread due to interregional contacts due to infective travelers, **d** suppression due to interregional contacts caused by the travels of vaccinated individuals in **a**

vaccinated individuals are spread by travels and cause social stirring, corresponding to the increase in H_c , which cuts the paths of infection spread. Thus, the social stirring effects due to traveling were found to depend on p_v in such a way as to enhance the spread of infection for the smaller p_v , and suppress it for the larger p_v . As the distribution of vaccines with a large H_c tends to result in suppressing the spread as shown in Figs. 5 and 6, maximizing H_c can be regarded as an effective policy to suppress the spread of infection.

To maximize H_c , we propose (1) and (2) as political vaccination strategies:

- (1) A region with a larger population is recommended if a single region is selected for vaccination.
- (2) If more than one region can be considered, the given quantity of vaccine should be distributed without intentional bias in a restricted region.

It is expected that the distribution of vaccines can be improved by increasing R_{vac} , the average effective reproduction number of vaccinated regions, for a smaller p_v . However, it should be noted that R_{ij} of each region j is not easy to use, because it tends to be unstable as in the target time range (April 2021 through March 2022), and it is not trustworthy to estimate its future value if there are some causes of change in people's social activities, such as Olympic games involving the studied regions. Furthermore, the less significant correlation, compared to H_c , of the average R_{vac} with the number of infection cases indicates a lower reliability of using effective reproduction numbers for suppressing the spread. The even lower performance of R_{vac} in Fig. 10 compared to Fig. 7 is inferred to be due to the extremely fast infection spread as B.1.617 is difficult to conquer, especially by slow vaccination, which may work if the spread is as slow as B.1.1.7. Thus, H_c can be regarded as more useful than effective reproduction numbers for improving the distribution of vaccines, because of its stable correlation with the number of infection cases.

On the other hand, as shown in Figs. 8 and 11, more frequent travel across the borders of prefectures represented by the larger α accelerates infection spread for a low vaccination pace, but the acceleration is moderate as p_v is improved, and then decelerates if p_v is further increased. However, the deceleration for a large p_v was not as significant as the acceleration with an increase in α for a small p_v . Thus, we should say “the risk due to travels can be suppressed” rather than “it is encouraged to travel” across prefectures by setting large p_v and H_c .

6 Conclusions

Mixing state-transition models, such as SEIR, its various extensions, and network models, is emerging as an established approach for obtaining unified models of interacting microscopic agents and macroscopic events in society [41–43]. In comparison, the method proposed in this study can be positioned as a method to model the networks of local societies to consider social stirring.

The findings of this study, that is, one that focused on vaccination in regions of the larger population as well as of the larger R_t tend to be effective for vaccination, and another that traveling causes not only enhancement but also suppression of infection expansion during the period of accelerated vaccination, coincide with the general tendencies shown in facts and studies that have worked on so far. These results partially support the reliability of this method in estimating the risks in local regions and the following discoveries regarding the tendencies of a group of regions, such as a nation, considering the interaction of micro-(among individuals within each region) and macro-(among regions) level interactions in society. Social stirring is a useful concept for explaining the findings of this study. The practical findings here are, in the third place, that a restricted quantity of vaccine can be used efficiently by maximizing conditional entropy. Fourth, travel across the borders of regions accelerates the spread of infection if the vaccine is distributed at a slower pace but may suppress it if the pace of vaccination is accelerated.

So far, the principle of staying with one's community has been shown to reduce the risk of travel by involving habitats in the target region in the process of embodying the research results into their own wisdom for living [44]. The findings of this study will be translated into political wisdom, including vaccination strategies.

Acknowledgements This study was supported by the Cabinet Secretariat of Japan both financially and through scientific communication. The computational basis of this study was partially supported by a grant from the JSPS KAKENHI 20K20482.

Author Contributions YO contributed to the design, implementation, and analysis in the research, SK to the conceptualization of the results. TM to the implementation in the research.

Funding Open Access funding provided by The University of Tokyo. This study was funded by Japan Science and Technology Corporation, JPMJPF2013, Yukio Ohsawa, JPMXS0118067246, Yukio Ohsawa, Japan Society for the Promotion of Science, 20K20482, Yukio Ohsawa, 23H00503, Yukio Ohsawa, MEXT Joint Programming Initiative A healthy diet for a healthy life, the Cabinet Secretariat of Japan.

Data Availability The data obtained and used for this paper are put in https://www.panda.sys.t.u-tokyo.ac.jp/LSEIRS_Ohsawa/Ohsawa_data_rev.zip. All data used in this study are included in the references.

Declarations

Conflict of Interest The authors declare that they have NO affiliations with or involvement in any organization or entity with any financial interest in the matter discussed in this manuscript.

Open Access This article is licensed under a Creative Commons Attribution 4.0 International License, which permits use, sharing, adaptation, distribution and reproduction in any medium or format, as long as you give appropriate credit to the original author(s) and the source, provide a link to the Creative Commons licence, and indicate if changes were made. The images or other third party material in this article are included in the article's Creative Commons licence, unless indicated otherwise in a credit line to the material. If material is not included in the article's Creative Commons licence and your intended use is not permitted by statutory regulation or exceeds the permitted use, you will need to obtain permission directly from the copyright holder. To view a copy of this licence, visit <http://creativecommons.org/licenses/by/4.0/>.

References

1. Ministry of Foreign Affairs in Japan. (2023). Phased measures for resuming cross-border travel. https://www.mofa.go.jp/ca/cp/page22e_000925.html
2. Aron, J. L., Schwartz, I. B., & Theor, J. (1984). Seasonality and period-doubling bifurcations in an epidemic model. *Journal of Theoretical Biology*, *110*(4), 665–679. [https://doi.org/10.1016/s0022-5193\(84\)80150-2](https://doi.org/10.1016/s0022-5193(84)80150-2)
3. López, L., & Rodó, X. V. (2021). A modified SEIR model to predict the COVID-19 outbreak in Spain and Italy: Simulating control scenarios and multi-scale epidemics. *Results in Physics*, *21*, 103746. <https://doi.org/10.1016/j.rinp.2020.103746>
4. Farzanegan, M. R., Gholipour, H. F., Feizi, M., Nunkoo, R., & Andargoli, A. E. (2021). International Tourism and Outbreak of Coronavirus (COVID-19): A cross-country analysis. *Journal of Travel Research*, *60*(3), 687–692. <https://doi.org/10.1177/0047287520931593>
5. Hu, D., Meng, N., Lou, X., Li, Z., Teng, Y., Zou, Y., & Wang, F. (2022). Significant correlation between tourism and COVID-19: Evidence from 178 countries and territories. *Journal of Infection in Developing Countries*, *16*(2), 283–290. <https://doi.org/10.3855/jidc.149295a>
6. Murano, Y., Ueno, R., Shi, S., et al. (2021). Impact of domestic travel restrictions on transmission of COVID-19 infection using public transportation network approach. *Science and Reports*, *11*, 3109. <https://doi.org/10.1038/s41598-021-81806-3>
7. Siegenfeld, A. F., & Bar-Yam, Y. (2020). The impact of travel and timing in eliminating COVID-19. *Communications on Physics*, *3*, 204. <https://doi.org/10.1038/s42005-020-00470-7>
8. Chinazzi, M., et al. (2020). The effect of travel restrictions on the spread of the 2019 novel coronavirus (COVID-19) outbreak. *Science*, *368*(6489), 395–400. <https://doi.org/10.1126/science.aba9757>
9. Ohsawa, Y., & Tsubokura, M. (2020). Stay with your community: Bridges between clusters trigger expansion of COVID-19. *PLoS ONE*, *15*(12), e0242766. <https://doi.org/10.1371/journal.pone.0242766>
10. Transportation Security Administration. (2021). TSA data TSA checkpoint travel numbers, <https://www.tsa.gov/coronavirus/passenger-throughput>
11. United States of America: WHO Coronavirus Disease (COVID-19) Dashboard With Vaccination Data. (2021). <https://covid19.who.int/region/amro/country/us>
12. Nwadiuko, J., & Bustamante, A. V. (2022). Little to no correlation found between immigrant entry and COVID-19 infection rates in the United States. *Health Affairs*, *41*(11), 1635–1644. <https://doi.org/10.1377/hlthaff.2021.01955.PMID:36343326.6a>
13. Chinazzi, M., et al. (2020). The effect of travel restrictions on the spread of the 2019 novel coronavirus outbreak. *Science*, *368*, 395–400. <https://doi.org/10.1126/science.aba97577a>
14. Harko, T., Lobo, F. S. N., & Mak, M. K. (2014). Exact analytical solutions of the Susceptible-Infected-Recovered (SIR) epidemic model and of the SIR model with equal death and birth rates. *Applied Mathematics and Computation*, *236*, 184–194. <https://doi.org/10.1016/j.amc.2014.03.030>. arXiv:1403.2160. Bibcode:2014arXiv1403.2160H. S2CID 14509477.
15. Beckley, R., et al. (2013). Modeling epidemics with differential equations, Tennessee State University Internal Report.; <https://www.tnstate.edu/mathematics/mathreu/filesreu/GroupProjectSIR.pdf>
16. Hethcote, H. (2000). The mathematics of infectious diseases. *SIAM Review.*, *42*(4), 599–653. <https://doi.org/10.1137/s0036144500371907>. Bibcode:2000SIAMR..42..599H.
17. Wu, J. T., Leung, K., & Leung, G. M. (2020). Nowcasting and forecasting the potential domestic and international spread of the 2019-nCoV outbreak originating in Wuhan, China: A modelling study. *Lancet*, *395*(10225), 689–697. [https://doi.org/10.1016/S0140-6736\(20\)30260-9](https://doi.org/10.1016/S0140-6736(20)30260-9)
18. Zhou, Y., Xu, R., Hu, D., Yue, Y., Li, Q., & Xia, J. (2020). Effects of human mobility restrictions on the spread of COVID-19 in Shenzhen, China: A modelling study using mobile phone data. *The Lancet Digital Health*, *2*(8), e417–e424. [https://doi.org/10.1016/S2589-7500\(20\)30165-5](https://doi.org/10.1016/S2589-7500(20)30165-5)
19. Chang, S., Pierson, E., Koh, P. W., Gerardin, J., Redbird, B., Grusky, D., & Leskovec, J. (2021). Mobility network models of COVID-19 explain inequities and inform reopening. *Nature*, *589*(7840), 82–87. <https://doi.org/10.1038/s41586-020-2923-3>
20. Kurahashi, S. (2021). Assessment of the Impact of COVID-19 Infections Considering Risk of Infected People Inflow to the Region", Int'l Workshop: Artificial Intelligence of & for Business (AI-Biz2021), JSAI International Symposia on AI, 3–3, 2021-11-15

21. Wilta, F., Chong, A. L. C., Selvachandran, G., Kotecha, K., & Ding, W. (2022). Generalized susceptible-exposed-infectious-recovered model and its contributing factors for analysing the death and recovery rates of the COVID-19 pandemic. *Applied Soft Computing*, 123, 108973. <https://doi.org/10.1016/j.asoc.2022.108973>
22. Jung, S., Kim, J. H., Hwang, S. S., Choi, J., & Lee, W. (2023). Modified susceptible–exposed–infectious–recovered model for assessing the effectiveness of non-pharmaceutical interventions during the COVID-19 pandemic in Seoul. *Journal of Theoretical Biology*. <https://doi.org/10.1016/j.jtbi.2022.111329>
23. Bjørnstad, O. N., Shea, K., Krzywinski, M., et al. (2020). The SEIRS model for infectious disease dynamics. *Nature Methods*, 17, 557–558. <https://doi.org/10.1038/s41592-020-0856-2>
24. Hansen, C. H., Michlmayr, D., Gubbels, S. M., Mølbak, K., & Ethelberg, S. (2021). Assessment of protection against reinfection with SARS-CoV-2 among 4 million PCR-tested individuals in Denmark in 2020: a population-level observational study. *Lancet*, 397(10280), 1204–1212. [https://doi.org/10.1016/S0140-6736\(21\)00575-4](https://doi.org/10.1016/S0140-6736(21)00575-4)
25. Tokyo Metropolitan Government Survey on the Number of Visitors, etc. (2019). <https://www.sangyo-rodo.metro.tokyo.lg.jp/toukei/tourism/h31-jittai/>
26. Japan Travel Bureau Foundation, Japanese people’s domestic travels (in Japanese Oct 2020) https://www.jtb.or.jp/wp-content/uploads/2020/10/nenpo2020_1-2.pdf
27. Travel Voice, Japanese Travel Trade News (2021). Domestic travelers in Japan are expected to double to 9.5 million in this year’s Golden Week, but to remain a 60% reduction over 2019 <https://www.travelvoice.jp/english/domestic-travelers-are-expected-to-double-to-9-5-million-in-this-year-s-golden-week-but-to-remain-a-60-reduction-over-2019>
28. CAPA Center for Aviation. (2021). Latest COVID-19 spike quashes Japan’s domestic air travel rebound, 19 Jan 2021 <https://centreforaviation.com/analysis/reports/latest-covid-19-spike-quashes-japans-domestic-air-travel-rebound-548928?>
29. Wagner, C. E., Saad-Roy, C. M., & Grenfell, B. T. (2022). Modelling vaccination strategies for COVID-19. *Nature Reviews Immunology*, 22, 139–141. <https://doi.org/10.1038/s41577-022-00687-3>
30. Gao, S., Teng, Z., Nieto, J. J., & Torres, A. (2007). Analysis of an SIR epidemic model with pulse vaccination and distributed time delay. *Journal of Biomedicine and Biotechnology*. <https://doi.org/10.1155/2007/64870>. PMC 2217597. PMID 18322563.
31. Ghostine, R., Gharamti, M., Hassrouny, S., & Hoteit, I. (2021). An extended SEIR model with vaccination for forecasting the COVID-19 pandemic in Saudi Arabia Using an Ensemble Kalman Filter. *Mathematics*. <https://doi.org/10.3390/math9060636>
32. Xu, Z., Wu, B., Topcu, U. (2021). Control strategies for COVID-19 epidemic with vaccination, shield immunity and quarantine: A metric temporal logic approach, <https://doi.org/10.1371/journal.pone.0247660>
33. Toyo Keizai Online. (2021). Coronavirus Disease (COVID-19) Situation Report in Japan., <https://toyokeizai.net/sp/visual/tko/covid19/en.html>
34. National Institute of Infectious Diseases. (2021). Epidemiological analysis of new mutant cases reported in Japan (1st report in Japanese). <https://www.niid.go.jp/niid/ja/diseases/ka/coronavirus/2019-ncov/10279-covid19-40.html>
35. Davies, N. G., et al. (2021). Estimated transmissibility and impact of SARS-CoV-2 lineage B.1.1.7 in England. *Science*. <https://doi.org/10.1126/science.abg3055>
36. Zhou, B., Thao, T. T. N., Hoffmann, D., et al. (2021). SARS-CoV-2 spike D614G change enhances replication and transmission. *Nature*. <https://doi.org/10.1038/s41586-021-03361-1>
37. Volz, E., Hill, V., McCrone, J., et al. (2021). Evaluating the effects of SARS-CoV-2 spike mutation D614G on transmissibility and pathogenicity. *Cell*. <https://doi.org/10.1016/j.cell.2020.11.020>
38. Korber, B., Fischer, W. M., Gnanakaran, S., et al. (2021). Tracking changes in SARS-CoV-2 spike: evidence that D614G increases infectivity of the COVID-19 virus. *Cell*. <https://doi.org/10.1016/j.cell.2020.06.043externalicon>
39. Syed, A. M., Ciling, A., & Taha, Y. (2021). Omicron mutations enhance infectivity and reduce antibody neutralization of SARS-CoV-2 virus-like particles. *PNAS*, 119(31), e2200592119. <https://doi.org/10.1073/pnas.2200592119>
40. Nihon Hoko Kyokai. (2021). *NHK news COV19 Prefectures Daily Data* https://www3.nhk.or.jp/n-data/opendata/coronavirus/nhk_news_covid19_prefectures_daily_data.csv

41. Liu, J., & Zhang, T. (2011). Epidemic spreading of an SEIRS model in scale-free networks. *Communications in Nonlinear Science and Numerical Simulation*, 16(8), 3375–3384. <https://doi.org/10.1016/j.cnsns.2010.11.019>
42. Karaivanov, A. (2020). A social network model of COVID-19. *PLoS ONE*, 15(10), 0240878. <https://doi.org/10.1371/journal.pone.0240878>
43. Groendyke, C., & Combs, A. (2021). Modifying the network-based stochastic SEIR model to account for quarantine: An application to COVID-19. *Epidemiologic Methods*, 10(1), 20200030. <https://doi.org/10.1515/em-2020-0030>
44. Ohsawa, Y., & Kondo, S. (2022). Regional workshop for policy implementation based on the stay with your community principles. *Procedia Computer Science*. <https://doi.org/10.1016/j.procs.2022.09.363>

Publisher's Note Springer Nature remains neutral with regard to jurisdictional claims in published maps and institutional affiliations.